Received Date: March 2025 Revised: April 2025 Accepted: June 2025

Nonrelativistic Analysis of Multi-Photon Ionization Using Volkov Solutions

[1]Subodh Kumar Yadav, [1]Kishori Yadav, [1,2] Saddam Husain Dhobi,

[1]Department of Physics, Patan Multiple Campus, Tribhuvan University, Lalitpur, Nepal

[2]Central Department of Physics, Tribhuvan University, Kirtipur, Kathmandu, Nepal

*Corresponding author: yadavsubodh002@gmail.com

Doi: https://doi.org/10.3126/ppj.v5i1.85847

Abstract

This article investigates the differential cross section (DCS) in laser-assisted hydrogen atom scattering, focusing on the impact of the scattering angle and momentum transfer. By analyzing the DCS trends for different photon interaction scenarios (N=0, N=1, N=2), we uncover the significant influence of external laser fields on scattering dynamics. The DCS decreases with increasing scattering angle, with forward scattering being enhanced and high-angle scattering suppressed. The Volkov wave function is employed to model the quantum state of the particles, providing insights into photon absorption and emission processes. The momentum transfer analysis reveals distinct scattering behaviors: for N=0, the DCS decreases sharply and stabilizes, while for N=1 and N=2, more complex patterns emerge, suggesting the effects of photon absorption and higher-order interactions. These findings enhance our understanding of laser-matter interactions and offer valuable insights for atomic collision physics and quantum control applications.

Keywords: Differential Cross Section, laser-assisted scattering, photon interaction, momentum transfer, Volkov wave function.

Introduction

It is well recognised that in order to eject a proton from its bounds state, both in an atom or a solid, the energy of a photon that strikes it must be greater than the electron's bound-state energy. However, at sufficiently high photon flux densities, the probability of simultaneous absorption of two or more photons increases. When the combined energy of these n absorbed photons exceeds the ionization potential (IP), the atom A is ionized by the light field, even if the energy of a single photon is much lower than the ionization potential (Delone & Krainov, 1999) as $A + n.\hbar\omega \longrightarrow A^{+} + e$. In the case with an unbound atom, as shown in the typical experimental scenario. According to momentum conservation between a residual ion and photo electron, the latter carries away everything but a minuscule percentage, or less than 1/2000 of the extra energy as $E_{ex} = n.\hbar w - IP.$

The study of multiphoton ionization (MPI) has advanced significantly since Einstein's description of light as an electromagnetic wave. Early theoretical predictions were made in the 1920s, and perturbation theories by Schrodinger, Dirac, and Geopart-Mayer explored

photon absorption and scattering processes (Dhobi et al., 2024). Experimental confirmations, such as the measurement of two-photon ionization in alkali and alkaline atoms, aligned with theoretical predictions (Delone & Krainov, 1999). With advances in laser technology, intense fields now enable the observation of multiphoton processes, such as multiphoton ionization, which are modeled using approaches like the Schrödinger equation and the Strong Field Approximation (SFA) (Kylstra et al., 2001; Long, 2012). Research also focuses on nondipole effects and final-state interactions in ionization (Kaminski & Krajewska, 2024; Trombetta et al., 1990), and the hybrid anti-symmetrized coupled channels method is used to analyze strong field ionization in multi-electron systems (Majety, 2015). The development of modified models like CV2− and MCV2− improves the description of multiphoton excitation by including resonant states (Guichard et al., 2007). Photon statistics and the Coulomb-Volkov approximation further refine predictions for electron distributions in strong laser fields (Mouloudakis & Lambropoulos, 2018; Arbó et al., 2008). The nonrelativistic framework for MPI has limitations, especially in high-energy regimes, requiring quantum electrodynamics (QED) treatments (Chen et al., 2003).

The thermal Hamiltonian of electrons in a laser field shows distinct interference and Coulomb-like behaviors in thermodynamic energy and potential, depending on the field amplitude and distance (Dhobi et al., 2022b). A study of laser-assisted thermal electron-hydrogen atom elastic scattering, using the first-born approximation and Volkov-Thermal wavefunctions, revealed that the differential cross-section (DCS) is higher for thermal electrons than for nonthermal ones, with destructive interference occurring only during photon absorption (Dhobi et al., 2024). Analysis of electron scattering by H_2 under various conditions showed that DCS increases with temperature and decreases with momentum and laser intensity, with circular polarization generally yielding higher DCS values than linear polarization (Shrestha et al., 2024). Electron-atom scattering in a linearly polarized laser field, using the first-order born approximation, indicated that stronger laser fields reduce energy shifts, while larger scattering angles and higher Bessel function orders decrease DCS, providing insights into atomic interactions under different conditions (Bohora et al., 2024). Finally, the DCS in a non-monochromatic laser-assisted thermal environment revealed that photon absorption results in higher DCS compared to photon emission due to atomic oscillation, with DCS behavior varying based on laser phase, polarization, and separation distance, offering valuable insights for quantum thermal machines and PEMFCs (Dhobi et al., 2025).

Methods and materials

This technique avoids any further approximation. We will look at an ordinary case: the ionisation of atoms of hydrogen in their ground state. For only one field parameter. We demonstrate that the method gives accurate energy spectra during ejected electrons, which are including many above-threshold ionisation peaks, as long as both of the following conditions are met simultaneously: (i) the photon energy is higher or equal to the ionisation potential, and (ii) the ionisation process is not fully saturated. Thus, this Coulomb-Volkov

treatment can be used to address ionisation of atoms or molecules caused by high-harmonic laser pulses that are now being created.

In nonrelativistic conditions, the wave function $\psi(\vec{r},t)$ interacting with an external electromagnetic field $\vec{F}(r,t)$ is given by the time dependent schrödinger eq^{n}.

$$\frac{i\partial\psi(\vec{r},t)}{\partial t} = \left[H_a + \vec{r}.\vec{F}(t)\right]\psi(r,t) \quad (1)$$

Where $H_a = -\frac{\nabla^2}{2} + V_a(\vec{r})$, $\vec{r}$ represents the electron's location relative to the nucleus, also known as the centre of mass. $\vec{F}(t)$ refers to the atom's external field. $V_a(\vec{r})$ depicts the interaction between an electron as well as the rest of the target. With a hydrogen-like target of nuclear charge, Z is simply:

$$V_a(\vec{r}) = -\frac{Z}{r} \quad (2)$$

The study is designed for an atom of hydrogen that is initially in the surrounding state. However, the model can be expanded to ions or atoms having just one valence electron by using an approach similar to that described by Jain and Tzoar (1978) for alkali-metal atoms. Thus, the field-free initial state is:

$$\emptyset_i(\vec{r},t) = \varphi_i(\vec{r})\exp(-i\varepsilon_i t) \quad (3)$$

Where $\varepsilon_i = -0.5$ is the energy of the ground state $\varphi_i(\vec{r})$ which is

$$\varphi_i(\vec{r}) = \frac{e^{-r}}{\sqrt{\pi}} \quad (4)$$

The unperturbed final continuum state $\phi_f^-(\vec{r},t)$ is the ingoing regular Coulomb wave function:

$$\phi_f^-(\vec{r},t) = \varphi_f^-(\vec{r})\exp(-i\varepsilon_f t) \quad (5)$$

Where $\phi_f^-(\vec{r})$ is continuum state of hydrogen normalized to $\delta(\vec{k}-\vec{k'})$; it is explicitly:

$$\varphi_f^- = (2\pi)^{\frac{3}{2}}\exp\left(+\frac{\pi v}{2}\right)\Gamma(1+iv)exp(\vec{ik}.\vec{r})_1F_1(-iv;1;-ikr-i\vec{k}.\vec{r}) \quad (6)$$

Where $\vec{k}$ is the electron's momentum, $\varepsilon_f = k^2/2$ is the eigenvalue energy of $\varphi_f^-(\vec{r})$, and $v = \frac{1}{k}$. The field-free Hamilton H_a has two eigen states: $\varphi_i(\vec{r})$ and $\varphi_f^-(\vec{r})$. A sine square envelope is used to represent the finite pulse duration. As a result, the external field around the atom is as follows:

$$\begin{cases}\vec{F}(t) = \vec{F}_0 sin(\omega t+\varphi)sin^2\left(\frac{\pi t}{\tau}\right) \ when\ t\in[0\ \tau] \\ \vec{F}(t) = \vec{0} \ \ elesewhere\end{cases} \quad (7)$$

τ represents the pulse's overall duration. In the following, we select ω=0.855a.u. to match the average high harmonics energy stated (Duchateau & Gayet, 2001). Although it is not very important when several oscillators are conducted inside (0,τ), all computations are made utilising a time systemic pulse, which means φ=π/2-ωτ/2. The laser's electric field is derived by the vector potential A (t), which reads:

$$\vec{A}(t) = \vec{A}(t_0) - \int_{t_0}^{t} dt' \vec{F}(t') \tag{8}$$

With the final state $\phi_f^-(\vec{r},t)$, one builds on ingoing Coulomb Volkov wave function $\chi_f^-(\vec{r},t)$. According to (Duchateau et al., 2000 and Kielpinski et al., 2014) it is,

$$\begin{cases} \chi_f^-(\vec{r},t) = \phi_f^-(\vec{r},t)\ \ L^-(\vec{r},t) \\ L^-(\vec{r},t) = \exp\left\{ i\vec{A}^-(t).\vec{r} - i\vec{k}.\int_t^t dt' \vec{A}^-(t') - \frac{i}{2}\int_t^t dt' \vec{A}^{-2}(t') \right\} \end{cases} \tag{9}$$

Where $\vec{A}^-(t)$ is the variation of $\vec{A}(t)$ over the time interval (τ, t) i.e.

$$\vec{A}^-(t) = \vec{A}(t) - \vec{A}(\tau) = -\int_\tau^t \vec{F}(t)dt \tag{10}$$

During an interaction time less than the original orbital period, a Coulomb-Volkov wave function provides an accurate depiction of the interaction system. In the Schrodinger image, the transition amplitude through the state i at t→-∞ towards the final condition f at t→-∞ can be evaluated at any time t as

$$T_{fi} = \langle \Psi_f^-(t) | \Psi_i^+(t) \rangle \tag{11}$$

Where $\Psi_f^-(\vec{r},t)$ and $\Psi_f^+(\vec{r},t)$ are the exact solutions of the equation (1) subject to the asymptotic conditions.:

$$\Psi_f^-(\vec{r},t) \xrightarrow[t\to+\infty]{} \phi_f(\vec{r},t) \tag{12a}$$

$$\Psi_i^+(\vec{r},t) \xrightarrow[t\to-\infty]{} \phi_i(\vec{r},t) \tag{12b}$$

In order to use the Coulomb-Volkov wave function $\chi_f^-(\vec{r},t)$, calculations are made with the so called prior form of the transition amplitude that is:

$$T_{fi}^- = \lim_{t\to-\infty} \langle \Psi_f^-(t) | \Psi_i^+(t) \rangle = \lim_{t\to-\infty} \langle \Psi_f^-(t) | \emptyset_i(t) \rangle \tag{13}$$

according to (12b) and because $\phi_1(\vec{r},t)$, $\phi_f^-(\vec{r},t)$are orthogonal, one may write:

$$T_{fi}^- = \lim_{t\to-\infty} \langle \Psi_f^-(t) | \emptyset_i(t) \rangle - \lim_{t\to-\infty} \langle \Psi_f^-(t) | \emptyset_i(t) \rangle = \int_{+\infty}^{-\infty} dt \frac{\partial}{\partial t} \langle \Psi_f^-(t) | \emptyset_i(t) \rangle \tag{14}$$

After a standard easy algebra, the expression (14) may be transformed into:

$$T_{fi}^- = -i\int_0^\tau dt \, \langle \Psi_f^-(t) | \vec{r}.\vec{F}(t) | \emptyset_i(t) \rangle \tag{15}$$

In perturbative conditions, one may substitute $\chi_f^-(\vec{r},t)$to $\Psi_f^-(\vec{r},t)$ in (12). Then, according to expression (3),(5) & (9). T_{fi}^- may be written as:

$$T_{fi}^- \cong T_{fi}^{CV2-} = -i\int_0^\tau dt \exp\left\{ i\left(\frac{k^2}{2} - \varepsilon_i\right)t + i\vec{k}.\int_0^\tau dt' \vec{A}^-(t') \right\} + \frac{i}{2}\int_\tau^t dt' \vec{A}^{-2}(t')$$
$$\times \int \vec{dr} \varphi_f^{-*}(\vec{r}) \exp\left(\vec{A}^{-2}(t).\vec{r}\right) \vec{r}.\vec{F}(t) \varphi_i(\vec{r}) \tag{16}$$

Let us introduce the useful functions:

$$h^-(t) = i\left(\frac{k^2}{2} - \varepsilon_i\right) + i\vec{k}.\vec{A}^-(t) + \frac{i}{2}\vec{A}^{-2}.(t) \tag{17}$$

$$f^-(t) = \exp\left\{ \int_\tau^t dt' h^-(t') \right\} \tag{18}$$

$$g^-(t) = \int \vec{dr} \varphi_f^{-*}(\vec{r}) \exp\left(-i\vec{A}^-(t).\vec{r}\right) \varphi_i(\vec{r}) \tag{19}$$

With the presentation (7) of the outside field $\vec{F}(t)$, the functions $h^-(t)$ and $f^-(t)$ can be computed analytically. Accurate numeric time integrations are possible even for more

intricate forms of $\vec{F}(t)$. Duchateau et al. (2000) provide a standard approach for obtaining a statistical expression for $g^{-}(t)$. According to (10), we have:

$$\frac{\partial}{\partial t} g^{-}(t) = i\int \overrightarrow{dr}\varphi_f^{-*}(\vec{r})\exp\left(-i\vec{A}^{-}(t).\vec{r}\right)\vec{r}.\vec{F}(t)\varphi_i(\vec{r}) \quad (20)$$

Thus, T_{fi}^{CV2-} may be written as:

$$T_{fi}^{CV2-} = -\int_0^{\tau} dt\ f^{-}(t)\frac{\partial}{\partial t}\ g^{-}(t) \quad (21)$$

Integrating by parts and bearing in mind that $\vec{A}^{-}(\tau) = \vec{0}$, one obtains:

$$T_{fi}^{CV2-} = f^{-}(0)g^{-}(0) - \int_0^{\tau} dt\ h^{-}(t)\ f^{-}(t)\ g^{-}(t) \quad (22)$$

The first item of the right-hand side in (22) is simply T_{fi}^{CV1-} (previous version of CV1) multiplied by a phase factor $f^{-}(0)$. For a true laser pulse, this value is zero, as there is no direct electric field present $\vec{A}(0) = \vec{0}$. To determine T_{fi}^{CV2-}., perform a simple mathematical time- integration throughout the pulse length. The angular distribution of expelled electrons can thus be expressed as:

$$\frac{\partial^2 P_{fi}^{CV2-}}{\partial E_k \partial \Omega_k} = k\left|T_{fi}^{CV2-}\right|^2 \quad (23)$$

In this equation, E_k and Ω_k represent the energy and direction of an expelled electron's impulse ($\vec{k}$). Integrating over Ω_k yields the energy distribution $\frac{\partial^2 P_{fi}^{CV2-}}{\partial E_k}$, whereas integrating over E_k yields the total probability $P_{fi}^{CV2-}$of ionising an atom with a single pulse. Our numerical method begins by diagonalising our hydrogen atom with a finite-sized Laguerre basis set, which results in a soft-walled potential atom in a box. We will enhance these approaches to calculate Raman scattering and Compton scattering. The Kramers-Heisenberg Waller matrix elements including electromagnetic coupling are used to calculate photon atom scattering cross-sections (Kielpinski et al., 2014).

$$H_e = (2mc^2)^{-1}e^2A^2 - (mc)^{-1}e\vec{p}.\vec{A} \quad (24)$$

However, we exclude the A^2 seagull component (the waller the matrix element) as it is only relevant at ≳KeV photon energy. Delserieys et al. (2008) define the Kramers-Heisenberg the matrix element as the transition polarisability $\propto_{ji}(\omega)$ between an initial state $|i; L_iS\rangle$ and a final state $|j; L_jS\rangle$ via a complete collection of intermediate states $|t; L_tS\rangle$. Here, we use simplified matrix elements with linear polarisation, such as

$$\propto_{ji}(\omega) \approx \sum_t C_{L_i, L_t, L_j}\left[\frac{(j\|z\|t)(t\|z\|i)}{\varepsilon_{ti}-\omega-i\frac{1}{2}\Gamma_{ti}(\omega)}\right] + \left[\frac{(j\|z\|t)(t\|z\|i)}{\varepsilon_{tj}-(-\omega)-i\frac{1}{2}\Gamma_{tj}(\omega)}\right] \quad (25)$$

Where $\varepsilon_{ab} = E_b - E_a$, all quantities above are in atomic units (a.u). $C_{0,1,0} = \frac{1}{3}$ whilst $C_{0,1,2} = \frac{1}{3}$. Each $\propto_{ji}(\omega)$ is calculated as a sum over intermediate states t which are either bound or pseudostates. When the intermediate state is bound state we compute an imaginary term (denoted Im_0) by the damping of the oscillator through the line width/s of the atomic bound state. If the intermediate state in eq (25) is a pseudo state then the linewidth is not included as continuum state don't have a physical linewidth. For (elastic) Rayleigh scattering of photon with frequency ω we have (Delserieys et al., 2008 and Langhoff et al., 1974)

$$\sigma_{e(\omega)} = \sigma_T \omega^4 |Re\ [\propto_{ii}(\omega)] + iIm_0 [\propto_{ii}(\omega)]|^2 \quad (26)$$

Where σ_T is the Thomsom scattering cross-section of a photon with free electron ($\sigma_T \approx 6.65 \times 10^{-25} cm^2$), while ω and $\propto_{ii}$ are both in a.u. The photoionization cross section is given by (Langhoff et al., 1974)

$$\sigma_{I(\omega)} = \sigma_T \frac{3}{2} c^3 \omega Im_1 [\alpha_{ii}(\omega)] \quad (27)$$

For (inelastic) Raman Scattering to state j

$$\sigma_{rij(\omega)} = \sigma_T \omega (\omega_j')^3 \left| Re[\propto_{ij}(\omega)] + iIm_0 [\propto_{ij}(\omega)] \right|^2 \quad (28)$$

with spontaneously emitted photon frequency $\omega_j' = \omega - \omega_{ij}$, the final process considered is that Compton Scattering which opens up for frequencies above threshold $\omega > |E_i|$ & analytically requires. The differential cross section to be integrated over all possible outgoing photon frequencies ω' (Drukarev et al., 2010)

$$\sigma_c(\omega) = \int_{\omega_{min}'}^{\omega_{max}'} \frac{d\sigma_c}{d\omega} \left| d\omega' \approx \sum_{(j;E_j>\Delta)} \sigma_{rij}(\omega) \right. \quad (29)$$

Where the largest emitted photon frequency $\omega_{max}' = \omega - |E_i|$, whilst the smallest ω_{min}' = 0

Result and Discussion

The Differential Cross Section is a key parameter in scattering theory that describes the probability of particles being scattered at specific angles during a collision. It provides detailed insights into the nature of the interaction between the particles involved. In the context of Figure 1 (where N is number of emitted photon), the DCS is plotted against the scattering angle for hydrogen atom scattering under the influence of a laser field. The figure reveals that the DCS decreases as the scattering angle increases, indicating a reduced likelihood of high-angle scattering. In laser-assisted scattering, the external laser field significantly modifies the interaction dynamics between the particles. The laser field introduces additional energy and momentum, which can affect the angular distribution of the scattered particles. This process alters the potential landscape experienced by the hydrogen atom, leading to changes in the scattering behavior. Specifically, the laser field often enhances forward scattering (small angles) while suppressing backward or large-angle scattering, as reflected in the decreasing DCS trend in Figure 1.

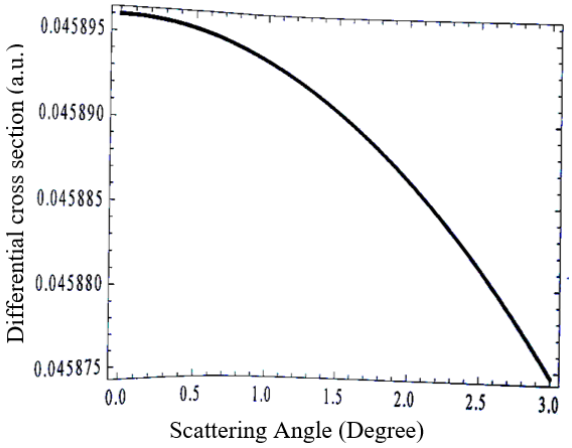

Figure 1: Variation of the differentials cross section with scattering angle for N=0

The Volkov wave function plays a crucial role in describing the quantum state of a particle in the presence of a laser field. It incorporates the effects of the electromagnetic field on the particle's motion, allowing for a more accurate description of laser-assisted scattering. The decreasing DCS with increasing scattering angle, as shown in Figure 1, can be attributed to the dynamic interaction potential shaped by the laser. The wave function helps model phenomena such as photon absorption or emission during scattering, which influence the angular distribution of scattered particles.

The observed decrease in DCS with scattering angle highlights several important physical implications. First, the dominance of forward scattering suggests that the laser field enhances the probability of small-angle scattering, a common feature in long-range interactions. Second, the reduction in DCS at larger angles reflects the redistribution of energy and momentum due to the laser's influence. Lastly, interference effects between particle waves, modified by the laser field, may further contribute to the suppression of high-angle scattering. These insights enhance our understanding of laser-matter interactions and their potential applications.

Figure 2 illustrates the variation of the differential scattering cross section (DCS) with momentum transfer for three cases: N=0, N=1, and N=2. The momentum transfer, denoted by qqq, represents the change in momentum of the incident electron as it interacts with the target. The DCS provides a measure of the probability of scattering at different values of qqq. The plot reveals distinct trends for each case (N=0, N=1, and N=2), reflecting variations in the scattering dynamics influenced by N, which might relate to photon absorption or emission in laser-assisted processes.

For N=0, the DCS initially decreases sharply as the momentum transfer increases. After this sharp decline, the DCS stabilizes and remains nearly constant over a range of momentum transfer values. Interestingly, beyond a specific threshold, the DCS begins to increase again, indicating a possible resonance or enhanced scattering probability. This behavior suggests that for N=0, the system undergoes minimal external perturbation, and the scattering

dynamics are primarily governed by intrinsic properties of the interaction. In the case of N=1, the DCS initially increases with an increase in momentum transfer. This rise is followed by a sharp decline as momentum transfer increases further. The sharp decrease in DCS for N=1 may indicate stronger interactions due to energy absorption or photon interaction, which alters the scattering probability. The sharper decline compared to N=2 highlights the distinct role that single-photon processes play in modifying the scattering dynamics.

For N=2, the DCS also shows an initial increase with rising momentum transfer, similar to N=1. However, the subsequent decline in DCS is less pronounced compared to N=1. This trend suggests that higher-order processes involving two photons contribute to stabilizing the scattering cross-section at larger momentum transfers. The reduced sharpness in the decline might be attributed to interference effects or energy redistribution over multiple scattering pathways. Comparing the three cases (N=0 N=1, and N=2), it is evident that N=0 exhibits a simpler scattering behavior with minimal external influence, while N=1 and N=2 show more complex dynamics due to laser-induced effects. The sharper decrease in DCS for N=1 compared to N=2 underscores the influence of the number of photons involved in the process, with higher photon counts leading to more gradual changes in the cross-section.

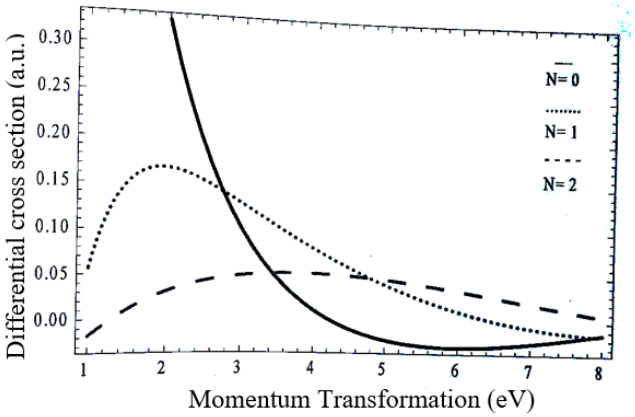

Figure 2: variation of differential cross section with momentum transformation for N=0, N=1 and N=2

The trends in DCS with momentum transfer provide valuable insights into the scattering mechanism under laser-assisted conditions. For N=0N = 0N=0, the scattering primarily reflects intrinsic interaction properties, while for N=1 and N=2, the laser field introduces additional complexities, such as energy exchange and interference effects. These findings have implications for understanding electron dynamics in external fields and could be applied to fields like laser-matter interaction studies, atomic collision physics, and quantum control. The nature of figure with emission of photon is similar to obtained (Dhobi et al., 2022a).

Conclusion

In this study, we have explored the differential cross section (DCS) as a key parameter in laser-assisted scattering processes involving hydrogen atoms. The DCS behavior with respect to scattering angle and momentum transfer reveals significant insights into the interaction dynamics influenced by external laser fields. Our findings demonstrate that the DCS decreases with increasing scattering angle, reflecting enhanced forward scattering and suppressed high-angle scattering due to the laser field's impact on the potential landscape. The Volkov wave function's role in accurately modeling these interactions highlights the influence of photon absorption and emission on the scattering process. Further analysis of the DCS variation with momentum transfer for different photon interaction cases (N=0, N=1, and N=2) reveals distinct trends. For N=0, the DCS decreases sharply with momentum transfer but stabilizes at higher values. In contrast, for N=1 and N=2, more complex dynamics emerge, with photon interaction leading to stronger variations in the DCS. The sharp decline in DCS for N=1 suggests more pronounced energy exchange, while the more gradual decrease for N=2 reflects the stabilizing effects of higher-order photon interactions. These insights are critical for understanding electron dynamics in laser-assisted scattering and have important implications for fields such as atomic collision physics and quantum control.

References

Delone, N. B., & Krainov, V. P. (1999). AC Stark shift of atomic energy levels. *Physics-Uspekhi*, *42*(7), 669.

Duchateau, G., & Gayet, R. (2001). Ionization of alkali-metal atoms by ultrashort laser pulses. *Physical Review A*, *65*(1), 013405.

Jain, M., & Tzoar, N. (1978). Compton scattering in the presence of coherent electromagnetic radiation. *Physical Review A*, *18*(2), 538.

Duchateau, G., Cormier, E., & Gayet, R. (2000). A simple non-perturbative approach of atom ionisation by intense and ultra-short laser pulses. *The European Physical Journal D-Atomic, Molecular, Optical and Plasma Physics*, *11*(2), 191-196.

Kielpinski, D., Sang, R. T., & Litvinyuk, I. V. (2014). Benchmarking strong-field ionization with atomic hydrogen. *Journal of Physics B: Atomic, Molecular and Optical Physics*, *47*(20), 204003.

Delserieys, A., Khattak, F. Y., Sahoo, S., Gribakin, G. F., Lewis, C. L. S., & Riley, D. (2008). Raman satellites in optical scattering from a laser-ablated Mg plume. *Physical Review A—Atomic, Molecular, and Optical Physics*, *78*(5), 055404.

Langhoff, P. W., Sims, J., & Corcoran, C. T. (1974). Stieltjes-integral approximations to photoabsorption and dispersion profiles in atomic helium. *Physical Review A*, *10*(3), 829.

Drukarev, E. G., Mikhailov, A. I., & Mikhailov, I. A. (2010). Low-energy K-shell Compton scattering. *Physical Review A—Atomic, Molecular, and Optical Physics*, *82*(2), 023404.

Duchateau, G., Cormier, E., & Gayet, R. (2003). Coulomb—Volkov approaches to atom ionization by short electromagnetic pulses. *Journal of Modern Optics*, *50*(3-4), 331-341.

Mouloudakis, G., & Lambropoulos, P. (2018). Revisiting photon-statistics effects on multiphoton ionization. *Physical Review A*, *97*(5), 053413.

Arbó, D. G., Miraglia, J. E., Gravielle, M. S., Schiessl, K., Persson, E., & Burgdörfer, J. (2008). Coulomb-Volkov approximation for near-threshold ionization by short laser pulses. *Physical Review A—Atomic, Molecular, and Optical Physics*, *77*(1), 013401.

Chen, J., Chen, S. G., & Liu, J. (2003). Quantum electrodynamic approach to multiphoton ionization in strong fields. *Journal of Physics B: Atomic, Molecular and Optical Physics*, *36*(8), 1559.

Majety, V. P., Zielinski, A., & Scrinzi, A. (2015). Photoionization of few electron systems: a hybrid coupled channels approach. *New Journal of Physics*, *17*(6), 063002.

Guichard, R., Bachau, H., Cormier, E., Gayet, R., & Rodriguez, V. D. (2007). In-depth analysis of Coulomb–Volkov approaches to ionization and excitation by laser pulses. *Physica Scripta*, *76*(4), 397.

Majety, N. V. V. P. (2015). *Strong field single ionization of atoms and small molecules* (Doctoral dissertation, lmu).

Trombetta, F., Basile, S., & Ferrante, G. (1990). Final State Interaction and Field Polarization Effects in the Multiphoton Ionization of Atoms. In *Atoms in Strong Fields* (pp. 457-471). Boston, MA: Springer US.

Kamiński, J. Z., & Krajewska, K. (2024). Multiphoton ionization distributions beyond the dipole approximation: Retardation versus recoil corrections. *arXiv preprint arXiv:2412.17996*.

Hu, H. (2011). *Multi-photon creation and single-photon annihilation of electron-positron pairs* (Doctoral dissertation, Ruprecht-Karls-Universität Heidelberg, Germany).

Kylstra, N. J., Joachain, C. J., & Dörr, M. (2001). Theory of multiphoton ionization of atoms. *Atoms, Solids, and Plasmas in Super-Intense Laser Fields*, 15-36.

Long, Z. (2012). Theoretical study of non-relativistic electron dynamics under intense laser fields. Dhobi, S. H., Yadav, K., Gupta, S. P., Nakarmi, J. J., & Koirala, B. (2022). Differential cross-section in the presence of a weak laser field for inelastic scattering. Ukrainian journal of physics, 67(4), 227-227.

Dhobi, S. H., Gupta, S. P., Yadav, K., Nakarmi, J. J., & Jha, A. K. (2024). Differential Cross Section With Volkov-Thermal Wave Function in Coulomb Potential. Atom Indonesia, 1(1).

Shrestha, C., Dhobi, S. H., & Shrestha, N. B. (2024). Strong-field nondipole approximation in laser-assisted thermal electron scattering. Insight Physics, 7(1), 641.

Bohora, R., Yadav, K., & Dhobi, S. H. (2024). Differential Cross-Sections and Energy Shifts in Electron-Atom Scattering Under Linearly Polarized Laser Fields. Journal of Optics and Photonics Research.

Dhobi, S. H., Nakarmi, J. J., Yadav, K., Gupta, S. P., Koirala, B., & Shah, A. K. (2022). Study of thermodynamics of a thermal electron in scattering. Heliyon, 8(12).

Dhobi, S. H., Yadav, K., Gupta, S. P., Nakarmi, J. J., & Jha, A. K. (2025). Non-monochromatic laser assist scattering in thermal environment. Journal of the Nigerian Society of Physical Sciences, 2345-2345.